ACS APPLIED MATERIALS & INTERFACES

www.acsami.org

Research Article

Rational Strategy for Space-Confined Atomic Layer Deposition

Ryoma Kamei, Takuro Hosomi, Masaki Kanai, Eisuke Kanao, Jiangyang Liu, Tsunaki Takahashi, Wenjun Li, Wataru Tanaka, Kazuki Nagashima, Katsuya Nakano, Koji Otsuka, Takuya Kubo, and Takeshi Yanagida*

Cite This: *ACS Appl. Mater. Interfaces* 2023, 15, 23931−23937

Read Online

ACCESS | Metrics & More | Article Recommendations | Supporting Information

ABSTRACT: Atomic layer deposition (ALD) offers excellent controllability of spatial uniformity, film thickness at the Angstrom level, and film composition even for high-aspect-ratio nanostructured surfaces, which are rarely attainable by other conventional deposition methodologies. Although ALD has been successfully applied to various substrates under open-top circumstances, the applicability of ALD to confined spaces has been limited because of the inherent difficulty of supplying precursors into confined spaces. Here, we propose a rational methodology to apply ALD growths to confined spaces (meter-long microtubes with an aspect ratio of up to 10 000). The ALD system, which can generate differential pressures to confined spaces, was newly developed. By using this ALD system, it is possible to deposit TiO_x layers onto the inner surface of capillary tubes with a length of 1000 mm and an inner diameter of 100 μm with spatial deposition uniformity. Furthermore, we show the superior thermal and chemical robustness of TiO_x-coated capillary microtubes for molecular separations when compared to conventional molecule-coated capillary microtubes. Thus, the present rational strategy of space-confined ALD offers a useful approach to design the chemical and physical properties of the inner surfaces of various confined spaces.

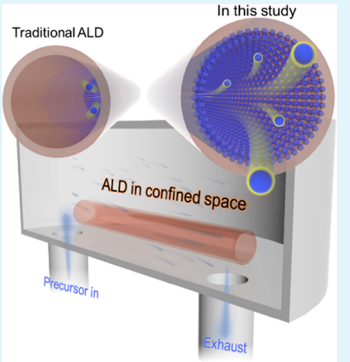

KEYWORDS: *atomic layer deposition, confined space, metal oxides, capillary tubes, high aspect ratio*

INTRODUCTION

Decorating artificially inner surface properties of confined spaces offers an interesting approach to design novel chemical events within spaces,[1−7] since an interaction between molecules and the surrounding inner surfaces dominates phenomena within confined spaces.[8−13] Although there are various surface decoration methods for inner surfaces of confined spaces,[14−16] inorganic solid decorations are particularly interesting approaches due to their thermal and chemical robustness and the elemental variation, which are rarely attainable with conventional organic surface modifications.[8,17,18] Among various inorganic solid surface decoration methods, atomic layer deposition (ALD) is one of powerful deposition techniques because of the excellent spatial deposition uniformity and atomic layer level thickness controllability even for complex nanostructured surfaces including needlelike high-aspect-ratio nanostructures, which are rarely depositable by other conventional methods.[19−35] In conventional ALD processes, the objects and/or targets to be deposited have been mostly various shaped substrates under open-top circumstances,[19,20] rather than the inner surface of confined spaces. Therefore, commercially available various ALD systems have been designed to operate under such open-top environments, where introducing precursors and/or waters into ALD chambers is easily performed without adding any special structures due to the relatively high flow conductance.[22]

In principle of ALD, supplying and/or removing precursors (or waters) on surfaces are critical processes to appropriately perform depositions.[26] Inherently, such supply and removal of precursors tends to be more difficult for confined spaces especially at high aspect ratios.[23] This is because the flow conductance for exchanging precursors tends to decrease as the aspect ratio of confined spaces increases.[36] Although the application of unique ALD techniques to confined spaces is clearly fascinating for designing chemical events within spaces, above inherent limitation of ALD hinders conventional ALD methodologies from performing depositions for inner surfaces of confined spaces. Here we propose a rational methodology to overcome above difficulty of ALD for confined spaces. We design our own ALD system, which can generate differential pressures to confined spaces. This ALD system enables us to successfully deposit a TiO_x layer onto the inner surface of capillary tubes with a length of 1000 mm and an inner diameter of 100 μm, where conventional ALD methods are not applicable. Furthermore, we show the superior thermal and

Received: February 14, 2023
Accepted: April 21, 2023
Published: May 8, 2023

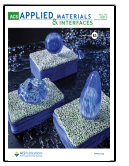

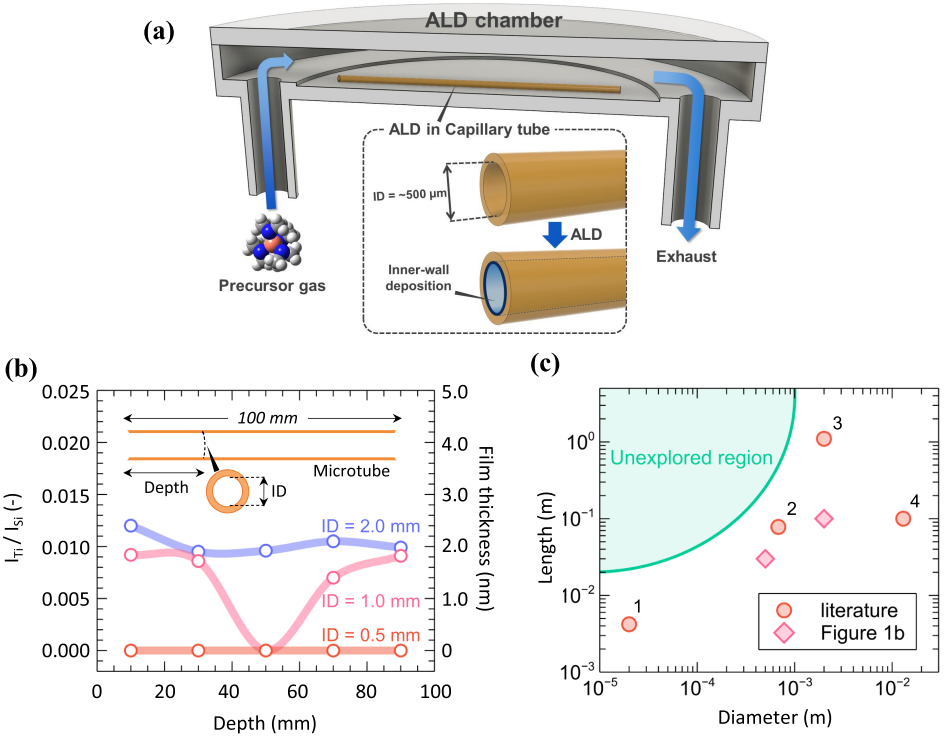

Figure 1. (a) Schematic of typical ALD system employed. (b) Spatial uniformity data of TiO_x depositions by conventional ALD system onto the inner surface of microtubes when varying inner diameters; the relative EDS intensity ratio of Ti/Si (I_{Ti}/I_{Si}) and the deposition thickness are shown. (c) Comparison between the present data and previous data [point 1 is from ref 1, point 2 is from ref 37, point 3 is from ref 38, and point 4 is from ref 39] on the depositable geometry of microtubes by conventional ALD.

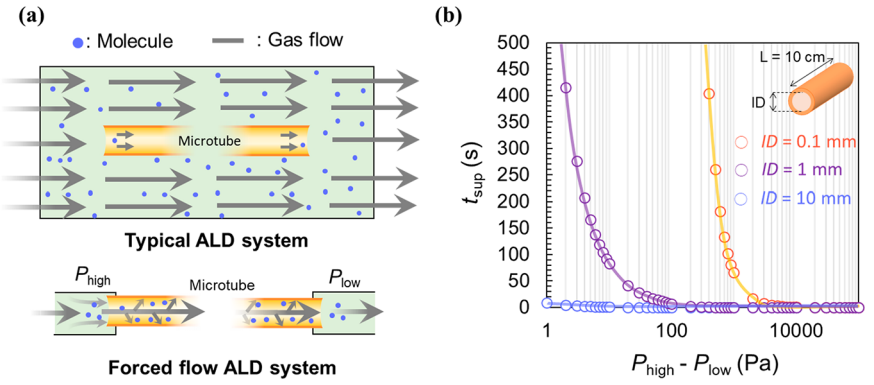

Figure 2. (a) Schematic of molecular behaviors into microtubes in typical ALD systems and/or in the forced-flow system proposed in this study, (b) Estimated molecular supply time t_{sup} of a microtube for various inner diameters (ID = 0.1, 1, or 10 mm) plotted against the differential pressures ($P_{high} - P_{low}$) of the inside and outside of the tube. The molecular supply time t_{sup} is defined as the time to transport the number of precursor molecules required to form a monolayer on the inner wall of the microtubes.

chemical robustness of such TiO_x-coated capillary tubes for molecular separations when compared to conventional molecule-coated capillary tubes.

RESULTS AND DISCUSSION

Figure 1a illustrates the schematic of experimental systems employed for conventional ALD system in the present experiments for microtubes. Microtubes with various inner diameters ID (ranging from 0.5 mm to 2 mm) and a length of 100 mm were placed into the ALD chamber. A Ti precursor (TDMAT) was used for these depositions. The deposition temperature was 150 °C. Figure 1b shows the spatial uniformity of TiO_x depositions onto the inner surfaces of microtubes when varying the size of the inner diameter. Since it is difficult to directly measure the TiO_x thin film thickness on the inner wall of microtubes with a length of 100 mm, we performed EDS measurements on the inner wall to measure the deposited Ti amount. A glass microtube was cut at several points, as illustrated in Figure 1b, and the EDS spectra at cross-sectional samples were measured. The EDS intensity ratio (I_{Ti}/I_{Si}) of Si (a component of the microtube body) and Ti was used as the index of spatial deposition uniformity, as shown in Figure 1b. In addition, the correlation between the I_{Ti}/I_{si} and the film thickness was extracted as shown in Figure S2. The correlation was obtained for TiO_x films on a flat SiO_x substrate. Typically, an EDS intensity ratio (I_{Ti}/I_{Si}) of 0.02 corresponds to a TiO_x thickness of 4.0 nm. The estimated film thickness data are also shown in Figure 1b. As clearly seen in Figure 1b,

https://doi.org/10.1021/acsami.3c01443
ACS Appl. Mater. Interfaces 2023, 15, 23931−23937

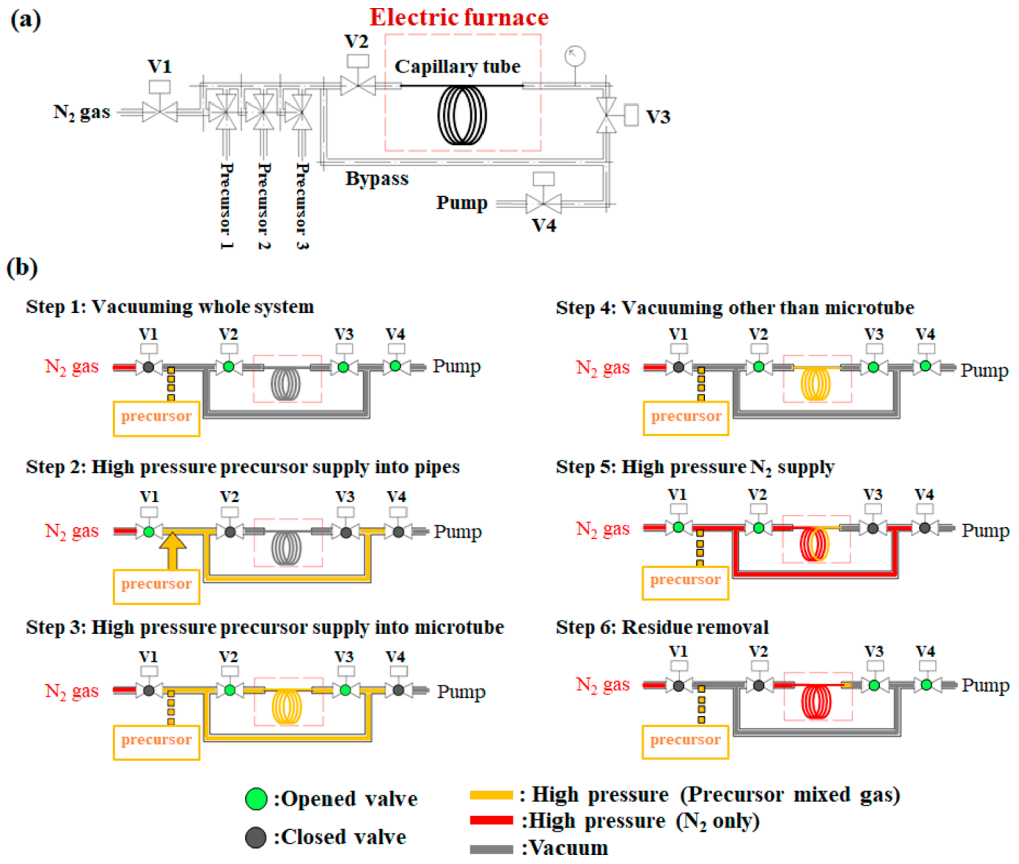

Figure 3. (a) Schematic of the developed ALD system, which can generate differential pressures for a forced flow. (b) Schematic of proposed ALD cycles and 6 steps to perform material supply and material removal for confined microtubes.

there is a significant size effect of inner diameter (ID) on the spatial uniformity of TiO_x depositions. In the case of microtube with an inner diameter of 2.0 mm, the TiO_x deposition was spatially uniform over the microtube length of 100 mm. However, such deposition uniformity tends to deteriorate as the inner diameter decreases. For the inner diameter of 1.0 mm, the TiO_x layer could be deposited only near both edges of microtubes, but not for the center part. When the inner diameter was smaller than 0.5 mm, the TiO_x could not be deposited at all for entire microtubes. Figure 1c shows the comparison between previous reports and the present data on ALD growth data within microtubes when varying the inner diameter and the length.[1,37−39] As seen in the figure, the ALD depositable geometry data of microtubes in previous works are consistent with the present data. The reason why there is difficulty in performing ALD growth within microtubes is clearly related to the low flow conductance of capillary microtubes, i.e., the supplied precursors cannot reach the center part of microtubes. Thus, there is an inherent limitation of conventional ALD methodology to deposit the inner surfaces of microtubes, where the space confinement effect dominates.

Conventional ALD processes for film depositions are performed in the presence of flows to deliver precursors and/or waters onto the target surfaces. However, as illustrated in Figure 2a, the necessity of such a flow process inherently limits the precursor supply into confined spaces like microtubes. This is because the flow conductance of microtubes tends to decrease as the inner diameter decreases, and a diffusion of precursors dominates the total precursor transportation. Based on Arnold's formula,[37] a diffusion is inversely proportional to pressure. Thus, within the framework of diffusion-rate-determining processes, depositing at lower pressures is required to enhance the deposition rate via increased diffusion constant. However, for microtubes, a precursor supply only via diffusion requires an extremely long time (e.g., estimated to be around 7000 s for a length of 100 mm and an inner diameter of 100 μm; see the calculation details in Figure S3), which is clearly not a realistic time range for cycled ALD experiments. One possible strategy to overcome this issue is to utilize differential pressures across microtubes, generating a forced flow. As shown in Figure 2b, we calculate a time to transport the number of precursor molecules required to form a monolayer on the inner wall of the microtubes (t_{sup}) as a function of differential pressures when varying the inner diameter of microtubes. For example, in the microtubes with ID = 0.1 mm, the differential pressures are required to be above around 500 Pa to generate a forced flow in the realistic deposition time range. Thus, it is possible to supply precursors into microtubes and remove them from microtubes by applying the appropriate differential pressures across microtubes. However, such experimental procedures are not feasible for conventional ALD systems. For this reason, we have developed an ALD system that can perform depositions for microtubes with the low flow conductance by generating forced flows.

Figure 3a shows the schematic of newly developed ALD system. This system is designed to be capable of applying the required differential pressures across microtubes during both processes including supplying precursors into microtubes and

https://doi.org/10.1021/acsami.3c01443
ACS Appl. Mater. Interfaces 2023, 15, 23931−23937

removing them from microtubes. As illustrated in Figure 3a, the pressure at both ends of the microtube can be independently controlled by valve operations, and relatively large differential pressures around 10^4 Pa can be generated for the microtube. The processes for one ALD cycle consist of 6 steps, as illustrated in Figure 3b. The first process (Step 1) is a whole evacuation of all ALD chamber components. The background pressure values are typically around 0.5 Pa. In Step 2, N_2 gas mixed with precursors is filled into pipes surrounding microtubes. In Step 3, by opening two values (V2 and V3), N_2 gas mixed with precursors is introduced from both ends of microtubes via the generated differential pressure. After this precursor deposition onto the inner surface of microtube (Step 3), residual precursors must be removed before the next precursor supply. In Step 4, by opening three valves (V2, V3, and V4), residual N_2 gas mixed with precursors is evacuated from all pipes surrounding microtube. However, due to the low flow conductance of the microtube, it is impossible to completely remove the residual precursor gas from the microtube, as illustrated in Figure 3b. To fully evacuate the residual precursors from microtube, in Step 5, pure N_2 gas is introduced into surrounding pipes by opening two valves (V1 and V2). Note that one side pipe of microtube near valve (V3) is intentionally closed to keep low pressure level (0.5 Pa). And then in Step 6, by opening two valves (V3 and V4), the residual precursors can be completely moved from microtubes by the N_2 forced flow via the pregenerated differential pressure. Thus, by utilizing the differential pressures across microtubes, supplying and/or removing precursors into/from microtube can be performed for ALD processes. Note that these experimental procedures utilizing differential pressures are essential to perform ALD growths for any confined spaces.

Figure 4 shows the application of developed ALD procedures to deposit TiO_x (Ti precursor: TDMAT) onto

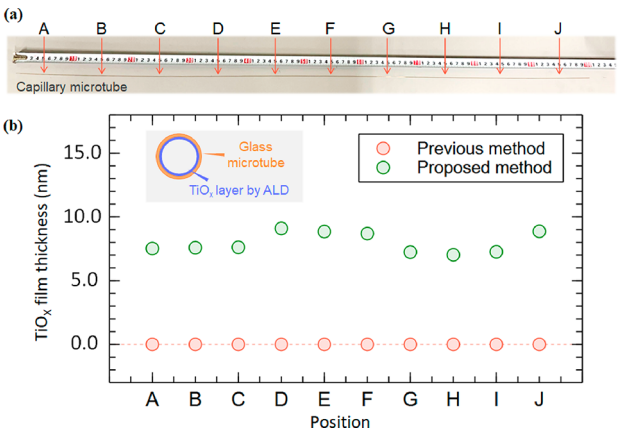

Figure 4. (a) Photograph of a capillary microtube. the spatial locations measured for EDS were highlighted as A–J. (b) Spatial uniformity of TiO_x deposition on the inner surfaces at various positions of the microtube.

the inner surface of microtube with the inner diameter of 100 μm and the length of 1000 mm (the aspect ratio: 10 000). Figure 4a shows the photograph of employed whole capillary microtube, and the measurements for deposition uniformity were performed at various positions A–J. Figure 4b shows the comparison between the developed ALD system and conventional ALD system for the TiO_x deposition onto the inner surface of microtubes. As clearly seen in Figure 4b, the sample prepared by conventional ALD system did not show any TiO_x growth in the microtube. On the other hands, spatially uniform TiO_x deposition can be observed for sample prepared by newly developed ALD system. These results highlight that our developed ALD system enables us to perform spatially uniform depositions on the inner surface of a long capillary microtube with a high aspect ratio of 10 000. Note that any previous ALD systems are not capable of depositing for such capillary microtubes.

Finally, we examine the applicability of fabricated capillary microtubes with TiO_x on the inner surface for thermally and chemically robust gas chromatography, as illustrated in Figure 5a. Figure 5b shows the comparison between the present capillary microtubes with TiO_x and a conventional molecularly decorated InertCap FFAP capillary column on the retention data using carboxylic acids (nonanoic acid, hexanoic acid). To examine the thermal robustness, we measured the thermal durability of both capillary columns. Figure 5c summarizes the thermal durability of the retention time when varying the thermal cycling time from room temperature to 350 °C. As can seen in the figure, the present capillary microtubes with TiO_x on the inner surface exhibited superior thermal stability when compared with the conventional FFAP capillary column. As the cycle number of thermal endurance increased, the retention time of FFAP significantly decreased, whereas the retention time of the present capillary microtubes with TiO_x could be maintained. Thus, the present capillary column coated by TiO_x via ALD can separate highly polar molecules with thermal robustness, which had been difficult using conventional molecule-coated capillary columns. Furthermore, our ALD method could be applied to the nanostructures formed within microtubes. We have previously constructed ZnO nanowires (ZnO-NW) on the inner wall of microtube capillary and implemented the capillary as a liquid phase separation column; the ZnO-NWs could adsorb phosphonic acids via electrostatic interaction.[40,41] However, the corrosion morphology of ZnO-NWs in the capillary column has been confirmed after exposures to acetate buffer in 4 h as seen in Figure 5d, e, and this corrosion has led to a loss of adsorption capacity for phosphonic acid (see the details in Figures S4 and S5). In contrast, ZnO-NWs coated by TiO_x via ALD could keep their specific adsorption capacity for phosphonic acids without corrosion of their inner-nanowire structures (Figure 5e). Briefly, the TiO_x coating via ALD improved the chemical robustness as a separation media of ZnO-NWs. Since this capillary column application is solely one example of various applications of the proposed ALD system to decorate the inner surface of confined spaces, the present rational strategy of space-confined ALD offers an approach to design the chemical and physical properties of various confined spaces.

CONCLUSION

We demonstrate a rational methodology to apply ALD depositions to confined spaces (meter-long microtubes of 100 μm inner diameter with an aspect ratio of up to 10 000). ALD system, which can generate differential pressure to confined spaces, was newly developed. This ALD system enables us to successfully deposit TiO_x layer onto the inner surface of capillary tubes with the length of 1000 mm and the inner diameter of 100 μm. Furthermore, we show the superior thermal robustness of such TiO_x-coated capillary tubes for molecular separations when compared to conventional molecule-coated capillary tubes. The present rational strategy

https://doi.org/10.1021/acsami.3c01443
ACS Appl. Mater. Interfaces 2023, 15, 23931–23937

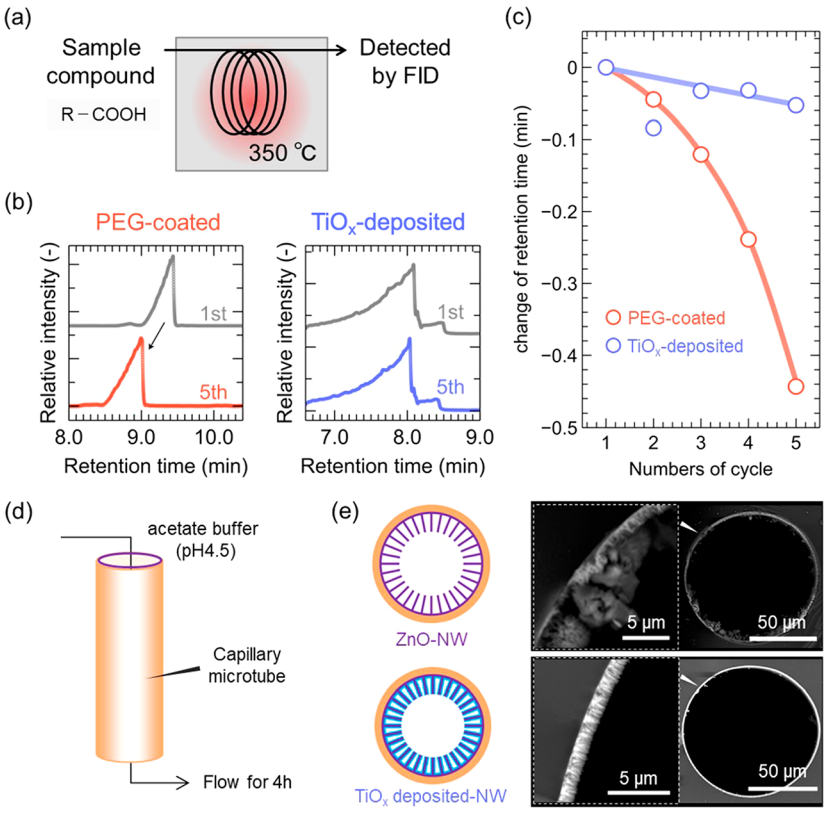

Figure 5. (a) Schematic of molecular separation experiments with ALD-deposited microtubes used as GC column. (b) Change in carboxylic acids peak retention time after five measurements on a PEG-coated column (left) and a TiO_x-deposited column (right). (c) Comparison between the present TiO_x-deposited column and conventional PEG-coated column on cycled retention time data. (d) Schematic of liquid-phase leaching resistance tests, and 10 mM acetate buffer (pH 4.5) was used as the liquid phase. (e) SEM images of a ZnO nanowire-arrayed capillary microtube (bare-NW) and a TiO_x-deposited ZnO nanowire-arrayed capillary microtube (TiO_x-deposited) after soaking with acetate buffer solution for 4 h.

of space-confined ALD offers a useful approach to design the chemical and physical properties of inner surfaces of various confined spaces.

METHODS

Materials. For glass microtubes, commercially available SiO_2 glass tubes (inner diameter/outer diameter = 2.0 mm/6.0 mm, 1.0 mm/4.0 mm, and 0.5 mm/3.0 mm) were used. For capillary microtubes, a polyimide-coated fused silica capillary tube (Molex 1068150023, inner diameter = 100 μm, outer diameter = 375 μm) was used. For the ALD TiO_x precursor, tetrakis(dimethylamino)titanium(IV) (TDMAT, purchased from Tri Chemical Laboratories Inc.) was used. N_2 gas (purity: 99.99%) was purchased from Taiyo Nippon Sanso Gas Co., Ltd. All chemicals in the GC measurements (nonanoic acid, hexanoic acid, nonanal, hexanal, 1-nonanol, 1-hexanol, and ethanol) were purchased from Tokyo Chemical Industry Co., Ltd., and used without further purifications. Adenosine monophosphate (AMP) was purchased from Sigma-Aldrich, and used as is.

Inner-tube Deposition with a Forced-Flow ALD System. The microtube was installed in the high differential pressure ALD shown in the Figure 3 with carbon ferrule joints. Prior to the deposition, the capillary tube was filled with N_2 at 8000 Pa and kept at 250 °C for 5 min. The following seven steps are performed sequentially for TDMAT and H_2O as the precursors to form one ALD cycle. Step 1: Evacuate the entire flow path for 1 min to reach 0.5 Pa. Step 2: Fill the outer flow path with 10 000 Pa precursor-mixed N_2. Step 3: Introduce precursor-mixed N_2 into the microtubes, and wait until the pressure stabilizes (within 30 s). Step 4: Evacuate the entire flow path for 1 min to roughly exhaust the precursor-mixed N_2 from the system. Step 5: Fill the path with clean N_2 at 10 000 Pa. Step 6: A vacuum is drawn from the downstream side to expel residual gas in the microtube (1 min). Step 7: Evacuate the entire flow path for 30 s to exhaust the gas from the microtubes. The system temperature was maintained at 250 °C throughout the cycle. It takes approximately 20 min to complete one cycle. The deposition rate of TiO_x at the center of the tube was calculated to be 0.04 nm/cycle in the case of the capillary tube (Molex 1068150023).

Inner-tube Deposition with a Typical ALD System. The microtube was placed in the chamber of a commercially available ALD system (Veeco Instruments Inc. Savannah S100) as shown in Figure 1a. The following five steps are performed to form one ALD cycle. Step 1: Evacuate the chamber (about 20 Pa) with 20 sccm N_2 flow. Step 2: Supply TDMAT by opening the precursor-supplying valve for 0.1 s. Step 3: Wait for 5 s with continuous N_2 flow. Step 4: Supply H_2O by opening the precursor-supplying valve for 0.015 s. Step 5: Wait for 5 s with continuous N_2 flow. Deposition rate of TiO_x on flat SiO_2 substrates is 0.04 nm/cycle.

Analysis of the Deposited Layer within the Microtube. The morphology of the TiO_x within microtubes was characterized by field emission scanning electron microscopy with energy dispersive X-ray spectroscopy (FESEM-EDS, JEOL JSM-7610F 30 kV) to quantify the atomic existing ratios. The microtubes were cut at 10 cm intervals to allow EDS measurements at each point. To evaluate the thickness of TiO_x films using EDS, calibration was performed using a standard sample. The ratio of Ti(Kα) to Si(Kα) characteristic X-ray intensities (I_{Ti}/I_{Si}) of a 500 μm thick TiO_x film deposited on a SiO_2 substrate by ALD was measured to obtain the relationship between TiO_x film thickness and I_{Ti}/I_{Si} value.

Gas Chromatography Analysis. The deposited microtubes were installed in a gas chromatograph system with a flame ionization detector (Shimadzu corp. GC-2030). A mixture of nonanoic acid, hexanoic acid, nonanal, hexanal, 1-nonanol, and 1-hexanol in ethanol (0.1 mM) was used as the standard sample mixture. The linear

https://doi.org/10.1021/acsami.3c01443
ACS Appl. Mater. Interfaces 2023, 15, 23931−23937

velocity of the carrier gas (He) was 2.0 cm/min. The inlet temperature is 400 °C. The column oven temperature was first held at 35 °C for 5 min, and then increased to 350 °C at a rate of 20 °C/min and held at that temperature for 10 min. InertCap FFAP (GL-Sciences Inc.) was used for the PEG-coated capillary column. The peaks were attributed to compounds by comparison of retention times with standard reagents.

Liquid-Phase Leaching Tolerance Tests. A bare-NW column (5.0 cm × 100 μm ID) was prepared by growing ZnO nanowire arrays on the inner wall of a capillary microtube by a method we recently reported.[41] The TiO_x-deposited column (5.0 cm × 100 μm ID) was prepared by depositing TiOx by ALD on the nanowires of the bare-NW column. Ten millimolar acetate buffer (pH4.5) was flowed into the columns for 4 h, and the morphology changes were observed by SEM. The SEM images before the liquid-phase leaching tolerance tests are shown in Figure 5e. Furthermore, The adsorption capacity of the capillary for phosphonic acid was evaluated by nanoliquid chromatography (nano-LC) after treatment with acetate buffer. A Nexera Micros (Shimadzu, Kyoto, Japan) series was used for nano-LC analysis. This system consisted of LC-Mikros (Shimadzu, Kyoto, Japan) as the pump, MU701 (GL Sciences, Tokyo, Japan) as the UV detector, a CHEMINERT as the sample injector, and CTO-20AC (Shimadzu, Kyoto, Japan) as the column oven. The detailed conditions are described in the Supporting Information.

■ ASSOCIATED CONTENT

Supporting Information

The Supporting Information is available free of charge at https://pubs.acs.org/doi/10.1021/acsami.3c01443.

Deposition results (Figure S1), correlation between EDS data and film thickness in TiO_x ALD depositions (Figure S2), estimated time for molecules to pass through the microtube when varying the pressure and the diameter (Figure S3), chemical robustness of TiO_x-coated microtubes with ZnO nanowires (Figures S4 and Figure S5) (PDF)

■ AUTHOR INFORMATION

Corresponding Author

Takeshi Yanagida − *Department of Applied Chemistry, Graduate School of Engineering, The University of Tokyo, Tokyo 113-8654, Japan; Institute for Materials Chemistry and Engineering, Kyushu University, Fukuoka 816-8580, Japan;* orcid.org/0000-0003-4837-5701; Email: yanagida@g.ecc.u-tokyo.ac.jp

Authors

Ryoma Kamei − *Department of Applied Chemistry, Graduate School of Engineering, The University of Tokyo, Tokyo 113-8654, Japan; Institute for Materials Chemistry and Engineering, Kyushu University, Fukuoka 816-8580, Japan*

Takuro Hosomi − *Department of Applied Chemistry, Graduate School of Engineering, The University of Tokyo, Tokyo 113-8654, Japan; JST-PRESTO, Kawaguchi, Saitama 332-0012, Japan;* orcid.org/0000-0002-5649-6696

Masaki Kanai − *Institute for Materials Chemistry and Engineering, Kyushu University, Fukuoka 816-8580, Japan*

Eisuke Kanao − *Graduate School of Pharmaceutical Sciences, Kyoto University, Kyoto 606-8501, Japan; National Institutes of Biomedical Innovation, Health and Nutrition, Ibaraki, Osaka 567-0085, Japan*

Jiangyang Liu − *Department of Applied Chemistry, Graduate School of Engineering, The University of Tokyo, Tokyo 113-8654, Japan;* orcid.org/0000-0001-5456-7705

Tsunaki Takahashi − *Department of Applied Chemistry, Graduate School of Engineering, The University of Tokyo, Tokyo 113-8654, Japan; JST-PRESTO, Kawaguchi, Saitama 332-0012, Japan;* orcid.org/0000-0002-2840-8038

Wenjun Li − *Department of Applied Chemistry, Graduate School of Engineering, The University of Tokyo, Tokyo 113-8654, Japan*

Wataru Tanaka − *Department of Applied Chemistry, Graduate School of Engineering, The University of Tokyo, Tokyo 113-8654, Japan*

Kazuki Nagashima − *Department of Applied Chemistry, Graduate School of Engineering, The University of Tokyo, Tokyo 113-8654, Japan; JST-PRESTO, Kawaguchi, Saitama 332-0012, Japan;* orcid.org/0000-0003-0180-816X

Katsuya Nakano − *Graduate School of Engineering, Kyoto University, Kyoto 615-8510, Japan*

Koji Otsuka − *Graduate School of Engineering, Kyoto University, Kyoto 615-8510, Japan*

Takuya Kubo − *Graduate School of Engineering, Kyoto University, Kyoto 615-8510, Japan;* orcid.org/0000-0002-9274-3295

Complete contact information is available at: https://pubs.acs.org/10.1021/acsami.3c01443

Notes

The authors declare no competing financial interest.

■ ACKNOWLEDGMENTS

This work was supported by KAKENHI. T.T., T.H., K.N., J.T., and T.Y. were supported by JST CREST, Japan. This work was performed under the Cooperative Research Program of "Network Joint Research Center for Materials and Devices" and the MEXT Project of "Integrated Research Consortium on Chemical Sciences".

■ REFERENCES

(1) Becker, J. S.; Suh, S.; Wang, S.; Gordon, R. G. Highly Conformal Thin Films of Tungsten Nitride Prepared by Atomic Layer Deposition from a Novel Precursor. *Chem. Mater.* **2003**, *15* (15), 2969−2976.

(2) Daiguji, H.; Yang, P.; Majumdar, A. Ion Transport in Nanofluidic Channels. *Nano Lett.* **2004**, *4* (1), 137−142.

(3) Green, Y.; Eshel, R.; Park, S.; Yossifon, G. Interplay between Nanochannel and Microchannel Resistances. *Nano Lett.* **2016**, *16* (4), 2744−2748.

(4) Wang, M.; Cheng, B.; Yang, Y.; Liu, H.; Huang, G.; Han, L.; Li, F.; Xu, F. Microchannel Stiffness and Confinement Jointly Induce the Mesenchymal-Amoeboid Transition of Cancer Cell Migration. *Nano Lett.* **2019**, *19* (9), 5949−5958.

(5) Ostler, D.; Kannam, S. K.; Frascoli, F.; Daivis, P. J.; Todd, B. D. Efficiency of Electropumping in Nanochannels. *Nano Lett.* **2020**, *20* (5), 3396−3402.

(6) Kitao, T.; Nagasaka, Y.; Karasawa, M.; Eguchi, T.; Kimizuka, N.; Ishii, K.; Yamada, T.; Uemura, T. Transcription of Chirality from Metal−Organic Framework to Polythiophene. *J. Am. Chem. Soc.* **2019**, *141* (50), 19565−19569.

(7) Daiguji, H. Ion Transport in Nanofluidic Channels. *Chem. Soc. Rev.* **2010**, *39* (3), 901−911.

(8) Yasui, T.; Rahong, S.; Motoyama, K.; Yanagida, T.; Wu, Q.; Kaji, N.; Kanai, M.; Doi, K.; Nagashima, K.; Tokeshi, M.; Taniguchi, M.; Kawano, S.; Kawai, T.; Baba, Y. DNA Manipulation and Separation in Sublithographic-Scale Nanowire Array. *ACS Nano* **2013**, *7* (4), 3029−3035.

(9) Rahong, S.; Yasui, T.; Yanagida, T.; Nagashima, K.; Kanai, M.; Klamchuen, A.; Meng, G.; He, Y.; Zhuge, F.; Kaji, N.; Kawai, T.;

Baba, Y. Ultrafast and Wide Range Analysis of DNA Molecules Using Rigid Network Structure of Solid Nanowires. *Sci. Rep.* **2014**, *4*, 5252.
(10) Wang, G.; Shi, G.; Wang, H.; Zhang, Q.; Li, Y. In Situ Functionalization of Stable 3D Nest-Like Networks in Confined Channels for Microfluidic Enrichment and Detection. *Adv. Funct. Mater.* **2014**, *24* (7), 1017−1026.
(11) Hu, W.; Liu, Y.; Chen, T.; Liu, Y.; Li, C. M. Hybrid ZnO Nanorod-Polymer Brush Hierarchically Nanostructured Substrate for Sensitive Antibody Microarrays. *Adv. Mater.* **2015**, *27* (1), 181−185.
(12) Rahong, S.; Yasui, T.; Yanagida, T.; Nagashima, K.; Kanai, M.; Meng, G.; He, Y.; Zhuge, F.; Kaji, N.; Kawai, T.; Baba, Y. Three-Dimensional Nanowire Structures for Ultra-Fast Separation of DNA, Protein and RNA Molecules. *Sci. Rep.* **2015**, *5*, 10584.
(13) Zhao, D.; Wu, Z.; Yu, J.; Wang, H.; Li, Y.; Duan, Y. Highly Sensitive Microfluidic Detection of Carcinoembryonic Antigen via a Synergetic Fluorescence Enhancement Strategy Based on the Micro/Nanostructure Optimization of ZnO Nanorod Arrays and in Situ ZIF-8 Coating. *Chemical Engineering Journal* **2020**, *383*, 123230.
(14) Primkulov, B. K.; Pahlavan, A. A.; Bourouiba, L.; Bush, J. W. M.; Juanes, R. Spin Coating of Capillary Tubes. *J. Fluid Mech.* **2020**, *886*, A30.
(15) Jeong, D.-H.; Xing, L.; Boutin, J.-B.; Sauret, A. Particulate Suspension Coating of Capillary Tubes. *Soft Matter* **2022**, *18* (42), 8124−8133.
(16) Jing, C.; Xiujian; Zhao; Han, J.; Zhu, K.; Liu, A.; Tao, H. A New Method of Fabricating Internally Sol−Gel Coated Capillary Tubes. *Surf. Coat. Technol.* **2003**, *162* (2), 228−233.
(17) Hu, W.; Lu, Z.; Liu, Y.; Chen, T.; Zhou, X.; Li, C. M. A Portable Flow-through Fluorescent Immunoassay Lab-on-a-Chip Device Using ZnO Nanorod-Decorated Glass Capillaries. *Lab Chip* **2013**, *13* (9), 1797−1802.
(18) Wang, G.; Li, K.; Purcell, F. J.; Zhao, D.; Zhang, W.; He, Z.; Tan, S.; Tang, Z.; Wang, H.; Reichmanis, E. Three-Dimensional Clustered Nanostructures for Microfluidic Surface-Enhanced Raman Detection. *ACS Appl. Mater. Interfaces* **2016**, *8* (37), 24974−24981.
(19) Knoops, H. C. M.; Potts, S. E.; Bol, A. A.; Kessels, W. M. M. 27 - Atomic Layer Deposition. In *Handbook of Crystal Growth*, second ed.; Kuech, T. F., Ed.; North-Holland: Boston, 2015; pp 1101−1134..
(20) Cremers, V.; Puurunen, R. L.; Dendooven, J. Conformality in Atomic Layer Deposition: Current Status Overview of Analysis and Modelling. *Applied Physics Reviews* **2019**, *6* (2), 021302.
(21) Elias, J.; Utke, I.; Yoon, S.; Bechelany, M.; Weidenkaff, A.; Michler, J.; Philippe, L. Electrochemical Growth of ZnO Nanowires on Atomic Layer Deposition Coated Polystyrene Sphere Templates. *Electrochim. Acta* **2013**, *110*, 387−392.
(22) Ren, Q.-H.; Zhang, Y.; Lu, H.-L.; Wang, Y.-P.; Liu, W.-J.; Ji, X.-M.; Devi, A.; Jiang, A.-Q.; Zhang, D. W. Atomic Layer Deposition of Nickel on ZnO Nanowire Arrays for High-Performance Supercapacitors. *ACS Appl. Mater. Interfaces* **2018**, *10* (1), 468−476.
(23) Chen, H.-S.; Chen, P.-H.; Kuo, J.-L.; Hsueh, Y.-C.; Perng, T.-P. TiO_2 Hollow Fibers with Internal Interconnected Nanotubes Prepared by Atomic Layer Deposition for Improved Photocatalytic Activity. *RSC Adv.* **2014**, *4* (76), 40482−40486.
(24) Zazpe, R.; Knaut, M.; Sopha, H.; Hromadko, L.; Albert, M.; Prikryl, J.; Gärtnerová, V.; Bartha, J. W.; Macak, J. M. Atomic Layer Deposition for Coating of High Aspect Ratio TiO_2 Nanotube Layers. *Langmuir* **2016**, *32* (41), 10551−10558.
(25) Gu, D.; Shrestha, P.; Baumgart, H.; Namkoong, G.; Abdel-Fattah, T. M. ALD Synthesis of Tube-in-Tube Nanostructures of Transition Metal Oxides by Template Replication. *ECS Trans.* **2009**, *25* (4), 191.
(26) George, S. M. Atomic Layer Deposition: An Overview. *Chem. Rev.* **2010**, *110* (1), 111−131.
(27) Gayle, A. J.; Berquist, Z. J.; Chen, Y.; Hill, A. J.; Hoffman, J. Y.; Bielinski, A. R.; Lenert, A.; Dasgupta, N. P. Tunable Atomic Layer Deposition into Ultra-High-Aspect-Ratio (>60000:1) Aerogel Monoliths Enabled by Transport Modeling. *Chem. Mater.* **2021**, *33* (14), 5572−5583.
(28) Su, C.-Y.; Wang, C.-C.; Hsueh, Y.-C.; Gurylev, V.; Kei, C.-C.; Perng, T.-P. Enabling High Solubility of ZnO in TiO_2 by Nanolamination of Atomic Layer Deposition. *Nanoscale* **2015**, *7* (45), 19222−19230.
(29) Becker, J. S.; Kim, E.; Gordon, R. G. Atomic Layer Deposition of Insulating Hafnium and Zirconium Nitrides. *Chem. Mater.* **2004**, *16* (18), 3497−3501.
(30) Gluch, J.; Rößler, T.; Schmidt, D.; Menzel, S. B.; Albert, M.; Eckert, J. TEM Characterization of ALD Layers in Deep Trenches Using a Dedicated FIB Lamellae Preparation Method. *Thin Solid Films* **2010**, *518* (16), 4553−4555.
(31) Ladanov, M.; Algarin-Amaris, P.; Matthews, G.; Ram, M.; Thomas, S.; Kumar, A.; Wang, J. Microfluidic Hydrothermal Growth of ZnO Nanowires over High Aspect Ratio Microstructures. *Nanotechnology* **2013**, *24* (37), 375301.
(32) Elam, J. W.; Routkevitch, D.; Mardilovich, P. P.; George, S. M. Conformal Coating on Ultrahigh-Aspect-Ratio Nanopores of Anodic Alumina by Atomic Layer Deposition. *Chem. Mater.* **2003**, *15* (18), 3507−3517.
(33) Perez, I.; Robertson, E.; Banerjee, P.; Henn-Lecordier, L.; Son, S. J.; Lee, S. B.; Rubloff, G. W. TEM-Based Metrology for HfO_2 Layers and Nanotubes Formed in Anodic Aluminum Oxide Nanopore Structures. *Small* **2008**, *4* (8), 1223−1232.
(34) Elam, J. W.; Xiong, G.; Han, C. Y.; Wang, H. H.; Birrell, J. P.; Welp, U.; Hryn, J. N.; Pellin, M. J.; Baumann, T. F.; Poco, J. F.; Satcher, J. H. Atomic Layer Deposition for the Conformal Coating of Nanoporous Materials. *J. Nanomater.* **2006**, *2006*, 1.
(35) Liu, K.-I.; Kei, C.-C.; Mishra, M.; Chen, P.-H.; Liu, W.-S.; Perng, T.-P. Uniform Coating of TiO_2 on High Aspect Ratio Substrates with Complex Morphology by Vertical Forced-Flow Atomic Layer Deposition. *RSC Adv.* **2017**, *7* (55), 34730−34735.
(36) Tison, S. A. Experimental Data and Theoretical Modeling of Gas Flows through Metal Capillary Leaks. *Vacuum* **1993**, *44* (11), 1171−1175.
(37) Nolan, M.; Povey, I.; Elliot, S.; Cordero, N.; Pemble, M.; Shortt, B.; Bavdaz, M. Uniform Coating of High Aspect Ratio Surfaces through Atomic Layer Deposition. In *Space Telescopes and Instrumentation 2012: Ultraviolet to Gamma Ray*; SPIE, 2012; Vol. *8443*, pp 1086−1093.
(38) Gong, T.; Hui, L.; Zhang, J.; Sun, D.; Qin, L.; Du, Y.; Li, C.; Lu, J.; Hu, S.; Feng, H. Atomic Layer Deposition of Alumina Passivation Layers in High-Aspect-Ratio Tubular Reactors for Coke Suppression during Thermal Cracking of Hydrocarbon Fuels. *Ind. Eng. Chem. Res.* **2015**, *54* (15), 3746−3753.
(39) Mishra, M.; Kei, C.-C.; Yu, Y.-H.; Liu, W.-S.; Perng, T.-P. Uniform Coating of Ta_2O_5 on Vertically Aligned Substrate: A Prelude to Forced Flow Atomic Layer Deposition. *Rev. Sci. Instrum.* **2017**, *88* (6), 065103.
(40) Kanao, E.; Nakano, K.; Kamei, R.; Hosomi, T.; Ishihama, Y.; Adachi, J.; Kubo, T.; Otsuka, K.; Yanagida, T. Moderate Molecular Recognitions on ZnO M-Plane and Their Selective Capture/Release of Bio-Related Phosphoric Acids. *Nanoscale Adv.* **2022**, *4* (6), 1649−1658.
(41) Kamei, R.; Hosomi, T.; Kanao, E.; Kanai, M.; Nagashima, K.; Takahashi, T.; Zhang, G.; Yasui, T.; Terao, J.; Otsuka, K.; Baba, Y.; Kubo, T.; Yanagida, T. Rational Strategy for Space-Confined Seeded Growth of ZnO Nanowires in Meter-Long Microtubes. *ACS Appl. Mater. Interfaces* **2021**, *13* (14), 16812−16819.

https://doi.org/10.1021/acsami.3c01443
ACS Appl. Mater. Interfaces 2023, 15, 23931−23937